

Accelerated Evolution of Maribavir Resistance in a Cytomegalovirus Exonuclease Domain II Mutant[∇]

Sunwen Chou^{1,2*} and Gail I. Marousek²

Division of Infectious Diseases, Oregon Health and Science University,¹ and Department of Veterans Affairs Medical Center,² Portland, Oregon

Received 15 August 2007/Accepted 10 October 2007

A human cytomegalovirus (CMV) UL54 *pol* exonuclease domain II mutation, D413A, found in a clinical specimen, conferred ganciclovir (GCV) and cidofovir resistance but not foscarnet resistance when incorporated into laboratory strain T2294. After several passages without drug, mutation was observed in five of eight plaques of T2294, and its plating efficiency under foscarnet was increased ~30-fold over that of a control strain. When T2294 was serially passed under maribavir (MBV), phenotypic changes and viral UL97 mutations were detected by passage 5, much earlier than previously reported for other CMV strains. By passage 15, mutations included two cases of H411Y, one each of H411L and H411N, three of T409M, five of V353A, and one of L397R. Five instances of codon 409 or 411 mutations evolved into double mutations including V353A. Marker transfer experiments showed H411N/Y/L to confer 9- to 70-fold-increased MBV resistance and combinations of H411L/Y and V353A to confer >150-fold-increased MBV resistance, but no GCV resistance. These findings are consistent with defective exonuclease activity of the *pol* D413A mutant T2294, leading to the accelerated evolution of UL97 mutations under MBV. This recapitulated the known resistance mutations V353A, L397R, and T409M; suggested their relative frequency; and identified new ones at codon 411. These UL97 mutations predict an MBV binding region overlapping the kinase ATP binding site and located upstream of known GCV resistance mutations. The existence of viable *pol* D413A mutants may facilitate the selection of additional drug resistance mutations *in vivo* and the study of these mutations *in vitro*.

The human cytomegalovirus (CMV) DNA polymerase, encoded by the viral UL54 *pol* gene, is the target of all currently licensed systemic anti-CMV drugs, namely, ganciclovir (GCV), foscarnet (FOS), and cidofovir (CDV). An increasingly diverse set of *pol* mutations has been linked to resistance to one or more of these drugs (3, 10). Most but not all mutations conferring FOS resistance map to *pol* regions II and III (codons 696 to 845); some mutations in region III also confer a low-grade GCV cross-resistance. Mutations in the exonuclease domains of *pol* (at codons 301, 408 to 413, and 501 to 545) are observed relatively frequently in association with GCV and CDV resistance (3). Of special interest are the aspartate residues 301 and 413 of the polymerase, which are located in exonuclease domains I and II, respectively. These highly conserved residues are present in the exonuclease domains of other alpha-like DNA polymerases (11). Previously described homologies (3) of codon 301 of CMV *pol* with codon 368 of herpes simplex virus (HSV) *pol* and codon 114 of bacteriophage RB69 *pol*, and of codon 413 of CMV *pol* with codon 471 of HSV *pol* and codon 222 of RB69 *pol*, are supported by the recently published crystal structure of the HSV DNA polymerase (20). The free carboxyl groups of these aspartate residues are proposed to be essential for magnesium binding and normal exonuclease activity, and HSV *pol* exonuclease mutations D368A and D471A were reported to prevent the recovery of viable recombinant viruses in a marker transfer system (11). Therefore, the recent finding of an analogous CMV *pol* muta-

tion, D413A, in sequences amplified directly from a clinical specimen (21) was unexpected and raised questions as to the viability and replication error rate of CMV strains containing this mutation. Marker transfer of D413A resulted in a mildly growth-impaired recombinant virus, T2294, exhibiting GCV and CDV resistance (21) but retaining FOS sensitivity. Here, we show evidence for an increased spontaneous mutation rate during propagation of T2294 and make use of this property to accelerate the discovery of UL97 mutations conferring resistance to the experimental benzimidazole L-riboside CMV UL97 kinase inhibitor drug maribavir (MBV) (1), which is currently in phase III clinical trials.

Emergence of the CMV UL97 serine-threonine kinase (13) as an antiviral drug target has drawn attention to its role in viral replication. CMV strains without a functioning UL97 gene show a severe growth defect (26) and an abnormal cytopathic effect (CPE) characterized by intranuclear inclusions containing excess pp65 (25). The same CPE is noted when wild-type CMV strains are treated with MBV, a potent UL97 inhibitor (1). The UL97 kinase likely influences virion morphogenesis, including such steps as encapsidation and nuclear egress, by acting on multiple viral and cellular substrates (16, 17, 22, 29). Antiviral activity has been noted in preliminary clinical trials of MBV (19), and no cross-resistance with current antiviral drugs has been observed to date (9). *In vitro* propagation of CMV strains under MBV has selected for several viral UL97 (1, 7) or UL27 (5, 15) mutations; there are no data yet on MBV resistance in treated human subjects. Further exploration of MBV resistance genotypes and mechanisms is needed to support the clinical development of this drug, thus prompting the present study.

* Corresponding author. Mailing address: VA Medical Center P31D, 3710 SW U.S. Veterans Hospital Road, Portland, OR 97239. Phone: (503) 273-5115. Fax: (503) 273-5116. E-mail: chous@ohsu.edu.

[∇] Published ahead of print on 17 October 2007.

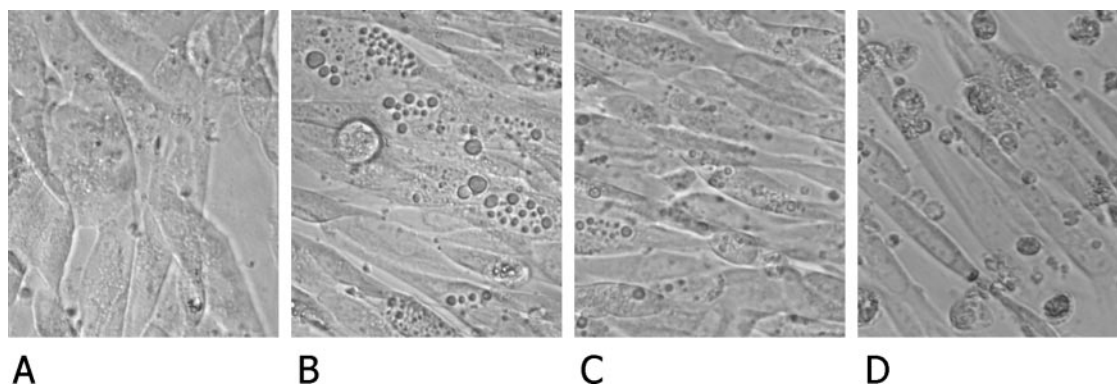


FIG. 1. Effect of MBV on CMV CPE. HEL fibroblasts 6 days after infection at a multiplicity of infection of 0.2 were photographed at an original magnification of $\times 20$ with phase contrast. (A) Control strain T2233 without MBV, showing normal (type 1) CPE. (B) Strain T2233 under $0.3 \mu\text{M}$ MBV, showing UL97-inhibited (type 2) CPE characterized by refractile nuclear inclusions increasing with advancing CPE. (C) Strain T2923 (H411L mutation) showing mixed type 1 and type 2 CPE under $10 \mu\text{M}$ MBV. (D) Strain T2903 (V353A and H411L mutations), showing advanced type 1 CPE with apoptotic cells but no nuclear inclusions in the presence of $20 \mu\text{M}$ MBV.

MATERIALS AND METHODS

Strains and cell cultures. Recombinant CMV strains T2211 (6), T2233 (6), T2241 (6), T2294 (21), and T1819 (3) have previously been described. The first three of these are baseline strains used as wild-type controls. T2211 was derived from strain AD169 by introduction of unique restriction sites (PmeI in *pol* and SmaI in UL97) and a secreted alkaline phosphatase (SEAP) expression cassette at US6, enabling the quantitation of viral growth by assaying the accumulation of SEAP activity in culture supernatants (6). Strain T2233 differs from strain T2211 by having a PmeI restriction site in UL97 instead of SmaI, while strain T2241 differs from T2211 by absence of the unique PmeI restriction sites in *pol*. Strain T2294 contains the *pol* mutation D413A and was derived from T2211 by PmeI digestion of T2211 DNA and recombination with a cotransfected 6.6-kb plasmid transfer vector (AD169 nucleotides [nt] 74828 to 81436; GenBank accession no. X17403) containing the *pol* mutation (21). Strain T1819 was constructed by a similar approach on a Towne strain background and contains the *pol* mutation D413E without a SEAP expression cassette (3). The viral strains were propagated in human foreskin fibroblast (HFF) or human embryonic lung (HEL) fibroblast cultures. Upon initial isolation, each strain was plaque purified three times, and DNA extracted from the first culture of the final picked plaque was sequenced through the entire *pol* gene to establish a baseline sequence for the strain, as originally published.

Transfer of *pol* mutation D413A to a CMV BAC. The *pol* mutation D413A was also transferred to the AD169-derived bacterial artificial chromosome (BAC) CMV clone pHB5 (2) by the *galK* selection and counterselection system using a conditionally recombinogenic *Escherichia coli* strain, SW102, and protocol as described previously (28). The BAC pHB5 was electroporated into SW102. The UL54 *pol* region of pHB5 was replaced by a *galK* expression cassette amplified using *galK* plasmid PCR primers (28) fused to 48- to 50-bp CMV sequences at the beginning and end of UL54 (5'-CGGTACAGATTCCTTGGACGGACAGACTGGCACGCAGGACAAGGACA and 5'-CACGTCGTCCTACGCGATACGGTCTCCCTTAACCGCGTCGCCGTTGCACG, respectively). This was accomplished by recombination in 42°C heat-induced SW102. Selection on galactose medium yielded BAC clone B7, which retained the intact XbaI restriction digest pattern of pHB5 and was checked by PCR for absence of the *pol* sequence that was replaced by the *galK* cassette. The *pol* mutation D413A was then introduced into B7 in heat-induced SW102 bacteria by electroporation of plasmid-derived transfer vector DNA containing a 6.6-kb *pol* region (nt 74828 to 81436 of the CMV strain AD169 sequence; GenBank accession no. X17403). Recombinant BACs were isolated by counterselection with 2-deoxygalactose as described previously (28) and again checked for an intact XbaI restriction digest pattern and sequenced throughout UL44 and UL54 *pol* for the presence of the intended mutation and absence of others. Live CMV was reconstituted by transfection of $2 \mu\text{g}$ BAC DNA extracted from SW102 cultures into subconfluent HFF monolayers in six-well culture plates, mediated by the Fugene 6 transfection reagent (Roche).

Serial propagation without drug. Plaque-purified strains T2211, T2294, and T1819 were serially propagated at weekly intervals at a multiplicity of infection of ~ 0.1 for 9 to 13 passages in HFF, followed by plating under agarose and picking eight individual plaques for resequencing of the *pol* gene (codons 300 to

1000) to determine if any sequence changes had occurred after serial passage. Sequencing was performed on PCR products of DNA extracted from the first culture of the individual plaques.

Plating efficiency under FOS. Cell-free viral stocks of T2211 and T2294 that had been propagated serially without drug were prepared. Twofold dilutions of these stocks were inoculated in 12-well-plate HFF cultures and incubated under agarose with or without $400 \mu\text{M}$ FOS (≥ 10 times the 50% inhibitory concentration [IC_{50}]), to compare the plating efficiencies of the two strains under drug, as previously described for HSV (27). After 7 to 10 days, the fibroblast monolayers were fixed and stained with Giemsa stain, and the plaques were counted at dilutions that contained 40 to 80 plaques per well. The plaque titer observed under drug divided by the titer observed without drug (plating efficiency) is used as an indicator of the rate of spontaneous mutation to drug resistance among different viral strains (27). The experiments were set up in duplicate on five separate dates, and the plating efficiency was calculated as the mean and standard error of the mean (SEM) of the results obtained on each of the five dates.

Selection of UL97 mutations under MBV. Strains T2294 and T2211 were serially propagated weekly as infected HEL fibroblasts starting at 0.1 to $0.3 \mu\text{M}$ MBV ($\sim 3 \times$ the IC_{50}), and the CPE was observed for the characteristic UL97-deficient phenotype (type 2) (Fig. 1B) of multiple refractile nuclear inclusions (25). When there was evidence of change toward the normal CPE (type 1) (Fig. 1A) of wild-type strains, the MBV concentration was increased stepwise to 10 to $15 \mu\text{M}$, and DNA extracts of infected cells were examined for sequence changes in UL97 by sequencing of PCR products. Serial changes in the UL97 genotype were monitored. Segregation of multiple mutations among different viral genomes was examined by cloning the PCR products into a topoisomerase-TA cloning vector (Topo TA cloning kit for sequencing; Invitrogen), followed by DNA sequencing of the TA clones.

Transfer of UL97 mutations to reference strains. UL97 mutations newly identified after viral propagation under MBV were transferred individually and in combination into a wild-type T2211 or T2241 background. Strain T2266 (7) was derived from T2211 by removal of the UL97 coding sequence from codon 536 to the end of the gene (codon 708) and had the inhibited (type 2) (Fig. 1B) UL97-defective CPE. The UL54 *pol* sequence of T2266 was rechecked for absence of changes from the baseline T2211 sequence. UL97 mutations were cloned into a plasmid transfer vector representing 4.7 kb of viral sequence (AD169 nt 139690 to 144436; GenBank accession no. X17403) in the UL97 region (6), and the digested plasmid DNA was transfected into T2266-infected HFF cultures using Fugene 6 transfection reagent (Roche). After a few passages, the viral CPE changed from the inhibited (type 2) to the normal (type 1) appearance (Fig. 1), signaling the outgrowth of recombinant virus incorporating the desired complete UL97 sequence containing the intended mutations. The recombinant viruses were then plaque purified three times and sequenced throughout UL97 to verify the presence of the complete UL97 coding sequence containing the desired mutations and without others. Alternatively, the desired UL97 mutation was transferred into strain T2241 using a previously described technique (6) of SmaI digestion of the parental strain DNA and cotransfection with the 4.7-kb transfer vector containing the UL97 mutation. Drug sensitivity was tested by a SEAP reporter yield reduction assay as previously described (6,

8). Based on the results of the prior studies, MBV assays were performed in HEL cell cultures and GCV assays in HFF cultures. The drug concentration required to reduce SEAP activity (relative light units emitted from a chemiluminescent substrate) in culture supernatants by 50% (IC_{50}) was determined and compared with those of the control strains T2211 and T2241 (7).

Structure comparisons. Related kinase structures identified by amino sequence homology were used to model the structure of the UL97 kinase and estimate the localization of MBV resistance mutations in relation to the kinase ATP binding and catalytic sites. Based on the location of the UL97 mutations affecting drug sensitivity, a putative MBV binding site was modeled. Publicly available resources for this purpose included the Basic Local Alignment Search Tool (BLAST; National Center for Biotechnology Information, <http://www.ncbi.nlm.nih.gov/BLAST>), CPH Models 2.0 (20a) (<http://www.cbs.dtu.dk/services/CPHmodels>), and MODELLER comparative protein structure modeling by satisfaction of spatial restraints, version 9.1 (<http://salilab.org/modeller>). Argus-Lab version 4.0.1 (M. A. Thompson, Planaria Software LLC, Seattle WA; <http://www.arguslab.com>) was used to generate structure images containing docked ATP and MBV molecules and to compute interatomic distances.

RESULTS

Viability of CMV *pol* D413A mutants. As previously reported (21), strain T2294 containing mutation D413A was constructed by recombination of PmeI-digested T2211 genomic DNA and a plasmid transfer vector DNA containing D413A and a silent base change at the adjacent codon 414 (TTG to CTT), which created a new AflIII restriction recognition site to distinguish it easily from the parental *pol* sequence. After three rounds of plaque purification, the complete UL44 DNA polymerase accessory protein, UL54 *pol*, and UL97 sequences of T2294 were determined, and these did not differ from those of the parental strain T2211 except for the changes in *pol* introduced by design. Strain T2294 was moderately growth attenuated (21), but at 7 to 8 days the cumulative growth approximated that of the wild-type control. Since the T2294 construction process did not involve viral propagation under any selective culture conditions, the absence of detectable extraneous mutations in its UL44, *pol*, and UL97 sequences was expected. However, because of the reported nonviability of the corresponding HSV D471A mutant (11) and the theoretical possibility that viability of T2294 is dependent on compensatory mutations in UL44 or *pol* that were selected during plaque purification and below the limits of detection by sequencing, an alternate construction process was used to prove the viability of the CMV *pol* D413A mutant. A CMV pHB5-derived BAC clone, B13, was created and was sequenced throughout UL44 and *pol* to verify the presence of mutation D413A and the absence of other mutations. Bacterially grown B13 DNA was transfected into HFF cultures, yielding live virus strain T2824 with a normal CPE at 13 days posttransfection. An infectivity titer of $>1 \times 10^6$ infectious units/ml of medium was attained 8 days after this initial culture was propagated. Infected-cell DNA was extracted, and the complete UL44 and *pol* sequences were the same as those of the parental BAC B13, including the D413A mutation. Because the mutant clonal BAC DNA yielded live virus T2824 in cell culture without any serial passage, it is concluded that no compensatory mutations are required for viability of the D413A mutant.

Sequence change after serial passage. Counting from initial plaque purification, strains T1819, T2294, and T2211 were serially propagated without drug for 9, 10, and 13 passages, respectively. Strain T1819 containing mutation D413E (3), derived from the Towne CMV strain, was included to compare

the effect of the D413A mutation with that of the more conservative D413E amino acid substitution. Individual plaques from the serially propagated strains were analyzed for their *pol* sequences from codon 300 to 1000, which includes the exonuclease and polymerase domains. All eight plaques sampled from each of strains T1819 and T2211 retained the same nucleotide and amino acid sequence as their respective strains at original isolation. In contrast, five of the eight plaques from strain T2294 at passage 10 showed a predicted amino acid change from the originally isolated T2294 and its parent T2211. The mutations were L445V, C592Y, and E858G, each found in one plaque, and loss of the D413A mutation in two plaques, causing a reversion to wild type at codon 413 but not at codon 414, where the continued presence of the CTT configuration indicated that the reversion of codon 413 to wild type was the result of a mutation and not simply a carryover of the parental strain T2211 from the original construction of strain T2294. The appearance of spontaneous mutation in plaques of the *pol* D413A mutant was further assessed by performing plating efficiency experiments under FOS.

Plating efficiency under FOS. Using a published method (27), the proportions of FOS-resistant plaques (plating efficiency) under a drug concentration of 400 μ M, ≥ 10 times the IC_{50} , were compared for the strains T1819, T2211, and T2294. This method is based on the assumption that the frequency of drug-resistant plaques in a viral pool is proportional to the mutation rate when the viruses have been similarly propagated without drug. As originally published (3, 21), neither strain T1819 nor T2294 showed any evidence for FOS resistance; their FOS IC_{50} s were lower than those for the parental strains. Therefore, no intrinsic FOS resistance is attributed to mutation at codon 413. For the plating efficiency experiments, virus stocks that were prepared after 10 passages (T1819 and T2294) or 13 passages (T2211) were used. The control strain T2211 was deliberately passed several more times to ensure that its total number of viral replication cycles would exceed those of the other strains. The observed plating efficiency was $0.45\% \pm 0.13\%$ (mean \pm SEM) for strain T2211, $0.13\% \pm 0.04\%$ for strain T1819, and $14\% \pm 4.1\%$ for strain T2294, based on five experiments per strain. By this assay, strain T2294 has a ~ 30 -fold increase in mutation rate compared to wild-type T2211 and a ~ 100 -fold increase compared to strain T1819. The difference between strains T2211 and T1819 is consistent with the previously reported hypersensitivity of T1819 to FOS (3).

Phenotypic change in cultures under MBV. The initial exposure of baseline CMV strains to MBV resulted in the UL97-inhibited type 2 CPE with refractile nuclear inclusions (Fig. 1B), which became more prominent as the CPE advanced. SEAP yield reduction assays showed IC_{50} s for MBV of $0.04 \pm 0.003 \mu$ M (mean \pm SEM) for strain T2294 and $0.11 \pm 0.03 \mu$ M for strain T2211. For strain T2294, after two passages under drug in HEL fibroblasts under a concentration of 0.1 μ M MBV, the partial appearance of normal (type 1) CPE was first noted in all six replicate experiments (M25 to M30) (Table 1). At passage 3, the drug concentration was changed to 0.3 μ M and increased thereafter as shown in Table 1. After several more passages, despite the increasing drug concentration, the CPE became mostly or entirely type 1 (Table 1), and the virus propagated easily under drug. In contrast, for the six experi-

TABLE 2. Segregation of mutations among PCR product clones (experiment M26)

Passage	No. of PCR product TA clones containing mutation(s):			
	L397R	H411Y	V353A and H411Y	None
9	9	3	0	2
13	7	1	5	0
26	15	0	8	0

ments done with strain T2211 (wild-type control), type 2 CPE was present throughout 10 passages under 0.3 μ M MBV.

Accelerated evolution of UL97 mutations. At passage 5 under MBV, DNA extracts were made of cells infected with strain T2294 and the PCR-amplified complete UL97 sequences were determined. This revealed a mutation at codon 409 or 411 (Table 1) in all six experiments, usually as a mixture with the wild-type sequence. The mutation T409M has previously been reported (7), while the mutations H411N, H411L, and H411Y are newly recognized. Retrospective analysis of extracts at passage 4 showed that the UL97 mutations were detectable by sequencing at that passage in only two of the six experiments. In addition, one experiment (M28) showed the contemporaneous detection of UL97 mutation D66Y at the first appearance of T409M and consistently thereafter. Pending further study, this is tentatively interpreted as a spontaneous mutation in T2294 that became coselected with T409M on the same genome. Upon escalation of the MBV concentration and further passage, additional UL97 mutations evolved in most cases. By passage 15, the most common outcome was to add the known mutation V353A (7) to a preexisting mutation at codon 409 or 411 (Table 1). In the most complex case (experiment M26), there was also the emergence of the known mutation L397R (1). Because none of the three mutations in this experiment reached 100% of the sequence population, cloning of UL97 PCR products from culture extracts at various passages was performed to determine the segregation of the mutations to different viral genomes. The results are shown in Table 2 and indicate the coexistence of viral genomes containing the mutation L397R, the mutation H411Y, or the combination of V353A and H411Y. The mutation H411Y appeared initially, followed by L397R and then the combination of V353A and H411Y, which is suggestive of a sequential evolution of mutations conferring higher levels of resistance. In contrast to the rapid evolution of UL97 mutations in strain T2294 propagated under MBV, similarly propagated control strain T2211 developed a partial H411Y mutation (Table 1) only at passage 10, and then in only one of six experiments. This is consistent with previous attempts to identify MBV resistance mutations by serial propagation of CMV clinical and laboratory strains under drug (1, 7), where mutations were not identified until passages 9 to 23.

Recombinant phenotyping of UL97 mutations. To determine the phenotypes conferred by specific UL97 mutations and combinations not previously studied, mutations were transferred to reference strains containing a SEAP reporter gene for viral quantitation. All of the UL97 mutants were derived from strain T2266 (indirectly from T2211), except for T2942 (H411N mutation), which was derived from strain

TABLE 3. Genotypes and phenotypes of recombinant viruses

Strain	UL97 mutation(s)	UL97 variation ^a	IC ₅₀ (μ M) ^b		MBV IC ₅₀ ratio ^c
			GCV	MBV	
T2211	None	H587Y	1.1 \pm 0.05	0.11 \pm 0.004	
T2233	None	None	1.1 \pm 0.04	0.12 \pm 0.003	
T2241	None	H587Y	1.2 \pm 0.08	0.10 \pm 0.004	
T2890	V353A	None	1.7 \pm 0.1	1.7 \pm 0.06	15
T2942	H411N	None	1.1 \pm 0.1	1.0 \pm 0.05	9
T2923	H411L	H587Y	0.77 \pm 0.08	7.6 \pm 0.5	69
T2893	H411Y	H587Y	0.5 \pm 0.02	1.3 \pm 0.04	12
T2903	V353A, H411L	H587Y	1.1 \pm 0.1	25 \pm 1.4	227
T2960	V353A, H411Y	H587Y	0.67 \pm 0.02	18 \pm 0.8	164

^a Amino acid change resulting from incorporation of unique *Sma*I restriction site.

^b Mean \pm SEM of at least 12 determinations done on three or more setup dates.

^c MBV IC₅₀ compared with that of baseline strain T2211.

T2241. Recombinant viruses containing the desired UL97 mutations were plaque purified, verified by sequencing throughout UL97, and tested for their level of sensitivity to GCV and MBV. The results are as shown in Table 3. The single UL97 mutations H411N, H411Y, and H411L conferred 9- to 70-fold-increased MBV resistance, which may be compared with published data showing mutations V353A and T409M to confer 15-fold and 80-fold-increased MBV resistance, respectively (7). The double mutations V353A in combination with either H411L or H411Y conferred >150-fold-increased resistance to MBV, which is comparable to the reported MBV resistance of the UL97 mutation L397R (1, 7). Thus, marker transfer recombinant phenotyping confirms the impression from observations during serial passage that the relatively lower levels of MBV resistance conferred by the initial mutations at codons 409 or 411 were subsequently replaced during serial passage by more resistant genotypes containing L397R or double mutations in combination with V353A. All of the UL97 mutants studied here remained sensitive to GCV.

Mapping of MBV resistance mutations to related kinase structures. The BLAST program identified the yeast GCN2 serine-threonine kinase (PDB identifiers 1zyc and 1zyd) (24) as the experimentally determined structure with the greatest amino acid homology to the UL97 kinase. In the kinase conserved domains I through VIb (12), corresponding to UL97 codons 326 to 465, the amino acid identity is 27%, with greater identities within domains I, II, and VIb themselves, thus enabling the identification of homologous residues within these domains (Fig. 2). The UL97 residues homologous to those in the GCN kinase structure are indicated in Fig. 3A and suggest that residues involved in MBV resistance (residues 353, 397, 409, and 411) are in the vicinity of the ATP binding and phosphotransfer domains (I, II, and VIb), including the invariant lysine (UL97 K355). Based on the alignment shown in Fig. 2A, a model of the UL97 kinase structure was constructed using the program CPH Models 2.0 and is shown in Fig. 3B and C as a ribbon cartoon of the protein backbone. The calculated model shows two loops of the protein backbone between residues 353 and 409 to 411, resulting in spatial proximity of residues 353 and 409 to 411 across a cleft. Residue 397 is more distant, near the turn of a loop.

When the ATP molecule is docked to the UL97 structure

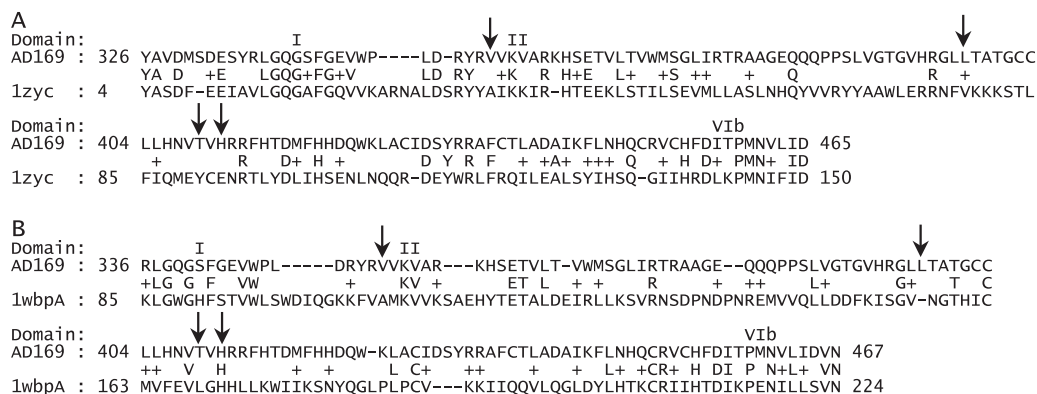


FIG. 2. Sequence alignments of UL97 and kinases of known structure. Alignments of UL97 amino acid residues of kinase domains I to VIb (12) with the corresponding residues of yeast GCN2 kinase (PDB 1zyc) (24) (A) and human SR protein kinase 1 (PDB 1wbp) (23) (B) are shown. These alignments were used to calculate the UL97 structure models shown in Fig. 3. Arrows indicate UL97 residues 353, 397, 409, and 411, which are involved in MBV resistance.

model (Fig. 3B), its projected position is analogous to that observed in the experimental structure of the GCN2 kinase (Fig. 3A). When MBV is docked to the same UL97 model structure (Fig. 3C), the projected position of the benzimidazole ring lies between residues 353 and 409 to 411 and is predicted to overlap that of ATP (Fig. 3B). When residue 397 is mutated (L397R) and the model structure is recomputed using the same program (CPH Models 2.0), greater separation

is found between residues 353 and 409 to 411; the distance between residues 353 and 409 increases from 5 to 14 angstroms, and the distance between residues 353 and 411 increases from 14 to 19 angstroms. This alters the docking of MBV. The proximity of the MBV molecule to residue 460 as shown in this model is compatible with the MBV hypersensitivity shown by the same M460V mutation that confers GCV resistance (7).

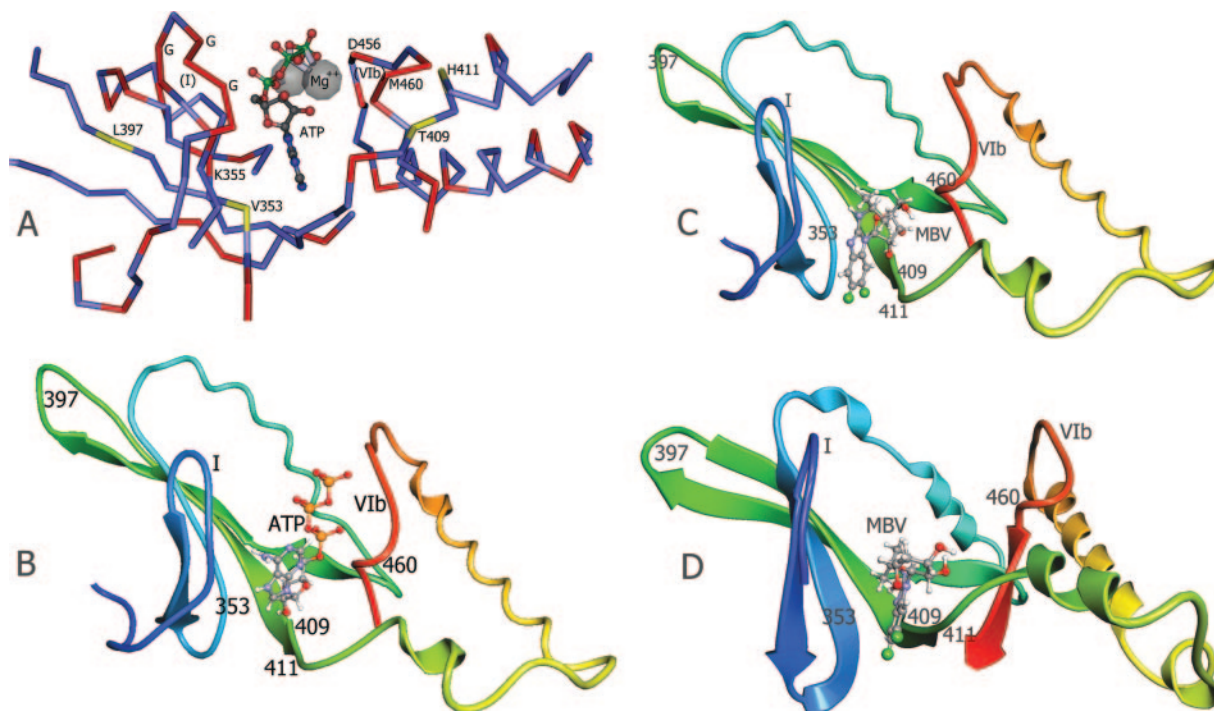


FIG. 3. Structure models of UL97 kinase ATP and MBV binding sites. (A) Corresponding residues of the UL97 sequence are labeled on the experimentally determined structure of yeast GCN2 kinase complexed to ATP (PDB 1zyd) (24). Residues identical in the two kinases are shown in red on the peptide backbone. G, conserved glycine residues in kinase domain I. (B) UL97 kinase ATP binding site structure model, based on the yeast GCN2 kinase structure (PDB 1zyc) (24) and the sequence alignment shown in Fig. 2A, as constructed by CPH Models 2.0. (C) MBV docked to the same UL97 structure model as above, guided by residues 353, 409, 411, and 460. (D) MBV docked to an alternative UL97 structure model based on the human SRPK1 structure (PDB 1wbp) (23) and the sequence alignment shown in Fig. 2B, as constructed by MODELLER v9.1. In the UL97 structure models, the ATP or MBV molecule was docked using ArgusLab v4 and structure displayed as a ribbon cartoon of protein backbone. Conserved kinase domains I and VIb and residues affecting MBV sensitivity are labeled.

An alternate serine kinase structure and modeling program were chosen to assess the similarity of the predicted MBV binding site. The human SR protein kinase SRPK1 (PDB 1wbpA) (23) sequence in domains I to VIb was aligned with the UL97 sequence as shown in Fig. 2B, with 22% sequence identity, and a structure model was computed using the MODELLER program. The resulting structure model (Fig. 3D) is closely comparable to the model shown in Fig. 3B and C despite differences in the structure template, sequence alignment detail, and modeling program. Again, residues 353 and 409 to 411 are on opposite sides of the benzimidazole ring, and residue 397 is located at the turn of a loop. As with the other model, the position of the docked MBV molecule is predicted to overlap that of docked ATP.

DISCUSSION

A CMV UL54 *pol* exonuclease domain II D413A mutation found in a clinical specimen, when transferred to a recombinant virus, resulted in an increased DNA replication error rate compatible with loss of exonuclease activity, although we did not isolate and purify the mutant enzyme to prove this directly. The increased error rate was used to accelerate the discovery of MBV resistance mutations by serial propagation under drug of a strain containing this mutation. UL97 mutations conferring MBV resistance were found clustered near the ATP binding and catalytic domains of the kinase, and structure models predict that MBV would interfere with ATP binding as its mechanism of action. Single and multiple UL97 mutations conferred levels of MBV resistance ranging from 9-fold to >150-fold, higher than generally observed with GCV resistance mutations. Continued exposure to MBV selected for very high levels of resistance, which may have clinical implications depending on the rapidity with which mutations are selected in vivo.

An increased mutation or DNA replication error rate in CMV attributable to an exonuclease domain mutation has not been reported. However, the analogous mutation D471A in the HSV DNA polymerase has been reported to have impaired exonuclease activity (18) and inability to be transferred into a viable recombinant virus (11). Exonuclease-defective HSV DNA polymerases appear to have an increased error rate, although it is not clear that the increased error rate alone prevents viral viability, since error-prone HSV exonuclease III domain mutants that were viable were constructed (14). The CMV D413A mutation was an unexpected finding in a clinical specimen (21) tested by PCR and sequencing in a diagnostic laboratory, without an accompanying viral culture. Evidence of viability therefore depended on the construction of a mutated recombinant virus, which showed only mild growth attenuation (21). Further evidence of viability was obtained by independently constructing a D413A mutant BAC clone and recovering live virus strain T2824 after transfecting the BAC DNA.

Three lines of evidence presented here indicate that the *pol* D413A mutant T2294 had an increased replication error rate: the finding of spontaneously mutated plaques, increased plating efficiency under FOS, and the accelerated evolution of MBV resistance mutations. This is in contrast to the *pol* D413E exonuclease II mutant T1819, also showing dual GCV-CDV resistance, which did not show an increased mutation rate,

possibly because of the conservative amino acid substitution. Although evolution of the D413A mutation that leads to an error-prone virus could be interpreted as a viral mechanism for facilitating drug resistance in vivo (as with human immunodeficiency virus), there is no evidence so far that this is a frequent occurrence in clinical CMV sequences from drug-treated patients.

The evolution of MBV resistance mutations in strain T2294 when propagated under drug was accelerated by at least five passages compared with the wild-type strain T2211 and markedly shortened the time needed to discover a variety of UL97 resistance-related mutations compared with previously published work (1, 7). This approach may be of general utility in assessing genetic mechanisms of resistance to new CMV therapies. After a few months of serial propagation, all previously described UL97 mutations conferring MBV resistance (L397R, V353A, and T409M) (1, 7) were recapitulated, and additional ones were identified at codon 411, along with combinations of V353A and other mutations that conferred very high-level MBV resistance. The multiple independent instances of mutations at codons 353, 409, and 411 suggest that these are the mutations most frequently selected after exposure to MBV and should be looked for in clinical specimens from subjects receiving prolonged MBV therapy. So far, the identified MBV resistance mutations in UL97 are all located upstream of known GCV resistance mutations, and no mutations have been found to confer resistance to both drugs. However, since the M460V mutation confers both GCV resistance and MBV hypersensitivity (7), it cannot be ruled out that other mutations in this vicinity may affect sensitivity to both drugs.

The specific mutations selected under MBV help to define a putative MBV binding locus in UL97. Because the mutated residues are close to highly conserved residues of serine-threonine kinases near the ATP binding site, known kinase structures can be used to model the MBV binding locus in UL97. Alignments of the UL97 sequence with those of other serine-threonine kinases (Fig. 2) reveal the expected high degree of homology within domains I, II, and VIb, such as the glycine residue in domain I at residues 338, 340, and 343; the invariant lysine in domain II at residue 355; and the aspartate and methionine residues in domain VIb at residues 456 and 460, respectively. The segment between domains II and VIb shows less homology and therefore less certainty with respect to the structure in this region where a high-grade MBV resistance mutation, L397R, is located. The segment is expected to play a major role in the specificity of action of MBV against UL97 but not host cell kinases. A consistent finding when modeling the UL97 kinase structure is for residues 353 and 409 to 411 to be in closer physical proximity than is suggested by their distance apart in the primary amino acid sequence. By using residues affecting MBV sensitivity to guide the docking of the drug to the estimated UL97 structure, both models for the MBV binding site place residues 353 and 409 to 411 on opposite sides of the benzimidazole ring. This could explain why double mutants involving both codons 353 and 411 show much higher resistance than either single mutant. Residue 397, which is not as accurately modeled because of imprecision in alignment with sequences of known structure, could indirectly affect the spatial relationship between residue 353 and others at 409 to 411 (Fig. 3C and D). Alternatively, if residue 397 is located more

proximally in the loop than is shown in these models, it could contact the MBV molecule directly, e.g., at the isopropylamino side chain. The models of MBV binding in Fig. 3 predict that it competes with the binding of ATP. Taken together with recent biochemical evidence (27a), these results show that interference with ATP binding may be proposed as the mechanism of action of MBV on UL97, a mechanism that would affect the action of UL97 on all of its potential substrates, including GCV, thus resulting in MBV-GCV antagonism (4) by preventing GCV phosphorylation. Information on the residues affecting MBV sensitivity will be useful in guiding the design of alternative UL97 inhibitors that lack cross-resistance.

ACKNOWLEDGMENTS

We thank Martin Messerle, Gabriele Hahn, and Ulrich Koszinowski for providing the pHB5 BAC and Donald Court and Neal Copeland for providing *E. coli* strain SW102 and the pGalK plasmid. Laura Van Wechel, Heather Lichy, and Daniel Mitchell provided technical assistance.

This work was supported by NIH grant AI39938 and by Department of Veterans Affairs Research Funds.

REFERENCES

- Biron, K. K., R. J. Harvey, S. C. Chamberlain, S. S. Good, A. A. Smith III, M. G. Davis, C. L. Talarico, W. H. Miller, R. Ferris, R. E. Dornsife, S. C. Stanat, J. C. Drach, L. B. Townsend, and G. W. Kozalka. 2002. Potent and selective inhibition of human cytomegalovirus replication by 1263W94, a benzimidazole L-riboside with a unique mode of action. *Antimicrob. Agents Chemother.* **46**:2365–2372.
- Borst, E. M., G. Hahn, U. H. Koszinowski, and M. Messerle. 1999. Cloning of the human cytomegalovirus (HCMV) genome as an infectious bacterial artificial chromosome in *Escherichia coli*: a new approach for construction of HCMV mutants. *J. Virol.* **73**:8320–8329.
- Chou, S., N. S. Lurain, K. D. Thompson, R. C. Miner, and W. L. Drew. 2003. Viral DNA polymerase mutations associated with drug resistance in human cytomegalovirus. *J. Infect. Dis.* **188**:32–39.
- Chou, S., and G. I. Marousek. 2006. Maribavir antagonizes the antiviral action of ganciclovir on human cytomegalovirus. *Antimicrob. Agents Chemother.* **50**:3470–3472.
- Chou, S., G. I. Marousek, A. E. Senters, M. G. Davis, and K. K. Biron. 2004. Mutations in the human cytomegalovirus UL27 gene that confer resistance to maribavir. *J. Virol.* **78**:7124–7130.
- Chou, S., L. C. Van Wechel, H. M. Lichy, and G. I. Marousek. 2005. Phenotyping of cytomegalovirus drug resistance mutations by using recombinant viruses incorporating a reporter gene. *Antimicrob. Agents Chemother.* **49**:2710–2715.
- Chou, S., L. C. van Wechel, and G. I. Marousek. 2007. Cytomegalovirus UL97 kinase mutations that confer maribavir resistance. *J. Infect. Dis.* **196**:91–94.
- Chou, S., L. C. Van Wechel, and G. I. Marousek. 2006. Effect of cell culture conditions on the anticytomegalovirus activity of maribavir. *Antimicrob. Agents Chemother.* **50**:2557–2559.
- Drew, W. L., R. C. Miner, G. I. Marousek, and S. Chou. 2006. Maribavir sensitivity of cytomegalovirus isolates resistant to ganciclovir, cidofovir or foscarnet. *J. Clin. Virol.* **37**:124–127.
- Gilbert, C., and G. Boivin. 2005. Human cytomegalovirus resistance to antiviral drugs. *Antimicrob. Agents Chemother.* **49**:873–883.
- Hall, J. D., K. L. Orth, K. L. Sander, B. M. Swihart, and R. A. Senese. 1995. Mutations within conserved motifs in the 3'-5' exonuclease domain of herpes simplex virus DNA polymerase. *J. Gen. Virol.* **76**:2999–3008.
- Hanks, S. K., A. M. Quinn, and T. Hunter. 1988. The protein kinase family: conserved features and deduced phylogeny of the catalytic domains. *Science* **241**:42–52.
- He, Z., Y. S. He, Y. Kim, L. Chu, C. Ohmstede, K. K. Biron, and D. M. Coen. 1997. The human cytomegalovirus UL97 protein is a protein kinase that autophosphorylates on serines and threonines. *J. Virol.* **71**:405–411.
- Hwang, Y. T., B. Y. Liu, D. M. Coen, and C. B. Hwang. 1997. Effects of mutations in the Exo III motif of the herpes simplex virus DNA polymerase gene on enzyme activities, viral replication, and replication fidelity. *J. Virol.* **71**:7791–7798.
- Komazin, G., R. G. Ptak, B. T. Emmer, L. B. Townsend, and J. C. Drach. 2003. Resistance of human cytomegalovirus to the benzimidazole L-ribonucleoside maribavir maps to UL27. *J. Virol.* **77**:11499–11506.
- Krosky, P. M., M. C. Baek, and D. M. Coen. 2003. The human cytomegalovirus UL97 protein kinase, an antiviral drug target, is required at the stage of nuclear egress. *J. Virol.* **77**:905–914.
- Krosky, P. M., M. C. Baek, W. J. Jahng, I. Barrera, R. J. Harvey, K. K. Biron, D. M. Coen, and P. B. Sethna. 2003. The human cytomegalovirus UL44 protein is a substrate for the UL97 protein kinase. *J. Virol.* **77**:7720–7727.
- Kuhn, F. J., and C. W. Knopf. 1996. Herpes simplex virus type 1 DNA polymerase. Mutational analysis of the 3'-5'-exonuclease domain. *J. Biol. Chem.* **271**:29245–29254.
- Lalezari, J. P., J. A. Aberg, L. H. Wang, M. B. Wire, R. Miner, W. Snowden, C. L. Talarico, S. Shaw, M. A. Jacobson, and W. L. Drew. 2002. Phase I dose escalation trial evaluating the pharmacokinetics, anti-human cytomegalovirus (HCMV) activity, and safety of 1263W94 in human immunodeficiency virus-infected men with asymptomatic HCMV shedding. *Antimicrob. Agents Chemother.* **46**:2969–2976.
- Liu, S., J. D. Knafels, J. S. Chang, G. A. Waszak, E. T. Baldwin, M. R. Deibel, Jr., D. R. Thomsen, F. L. Homa, P. A. Wells, M. C. Tory, R. A. Poorman, H. Gao, X. Qiu, and A. P. Seddon. 2006. Crystal structure of the herpes simplex virus 1 DNA polymerase. *J. Biol. Chem.* **281**:18193–18200.
- Lund, O., M. Nielsen, C. Lundegaard, and P. Worning. 2002. CPHmodels 2.0: X3M, a computer program to extract 3D models, abstr. A102. CASP5 conference.
- Marfori, J. E., M. M. Exner, G. I. Marousek, S. Chou, and W. L. Drew. 2007. Development of new cytomegalovirus UL97 and DNA polymerase mutations conferring drug resistance after valganciclovir therapy in allogeneic stem cell recipients. *J. Clin. Virol.* **38**:120–125.
- Marschall, M., M. Freitag, P. Suchy, D. Romaker, R. Kupfer, M. Hanke, and T. Stamminger. 2003. The protein kinase pUL97 of human cytomegalovirus interacts with and phosphorylates the DNA polymerase processivity factor pUL44. *Virology* **311**:60–71.
- Ngo, J. C., S. Chakrabarti, J. H. Ding, A. Velazquez-Dones, B. Nolen, B. E. Aubol, J. A. Adams, X. D. Fu, and G. Ghosh. 2005. Interplay between SRPK and Clk/Sty kinases in phosphorylation of the splicing factor ASF/SF2 is regulated by a docking motif in ASF/SF2. *Mol. Cell* **20**:77–89.
- Padyana, A. K., H. Qiu, A. Roll-Mecak, A. G. Hinnebusch, and S. K. Burley. 2005. Structural basis for autoinhibition and mutational activation of eukaryotic initiation factor 2alpha protein kinase GCN2. *J. Biol. Chem.* **280**:29289–29299.
- Prichard, M. N., W. J. Britt, S. L. Daily, C. B. Hartline, and E. R. Kern. 2005. Human cytomegalovirus UL97 kinase is required for the normal intranuclear distribution of pp65 and virion morphogenesis. *J. Virol.* **79**:15494–15502.
- Prichard, M. N., N. Gao, S. Jairath, G. Mulamba, P. Krosky, D. M. Coen, B. O. Parker, and G. S. Pari. 1999. A recombinant human cytomegalovirus with a large deletion in UL97 has a severe replication deficiency. *J. Virol.* **73**:5663–5670.
- Sarisky, R. T., T. T. Nguyen, K. E. Duffy, R. J. Wittrock, and J. J. Leary. 2000. Difference in incidence of spontaneous mutations between herpes simplex virus types 1 and 2. *Antimicrob. Agents Chemother.* **44**:1524–1529.
- Truesdale, A. T., K. K. Biron, B. P. Ellis, W. H. Miller, and E. R. Wood. 2007. Mode of inhibition studies with MBV and the CMV kinase UL97, abstr. 10.27. 32nd Int. Herpesvirus Workshop, Asheville, NC.
- Warming, S., N. Costantino, D. L. Court, N. A. Jenkins, and N. G. Copeland. 2005. Simple and highly efficient BAC recombineering using galK selection. *Nucleic Acids Res.* **33**:e36.
- Wolf, D. G., C. T. Courcelle, M. N. Prichard, and E. S. Mocarski. 2001. Distinct and separate roles for herpesvirus-conserved UL97 kinase in cytomegalovirus DNA synthesis and encapsidation. *Proc. Natl. Acad. Sci. USA* **98**:1895–1900.